J Am Oil Chem Soc (2010) 87:1137–1143
DOI 10.1007/s11746-010-1604-z

ORIGINAL PAPER

Blooming in Cocoa Butter Substitutes Based Compound Chocolate: Investigations on Composition, Morphology and Melting Behavior

Fengyan Wang · Yuanfa Liu · Liang Shan · Qingzhe Jin · Xingguo Wang · Lingling Li

Received: 29 October 2009 / Revised: 7 March 2010 / Accepted: 12 May 2010 / Published online: 12 June 2010

Abstract To provide a comprehensive analysis on the development of bloom on cocoa butter substitutes based compound chocolate, the morphology, chemical composition and melting behavior were examined. Atomic force microscopy (AFM), scanning electric microscopy (SEM), and polarized light microscopy (PLM) measurements were carried out to study the morphological properties of chocolate. AFM analyses showed a crystal growth which was confirmed by using PLM. SEM revealed that the crystal network of fresh chocolate disappeared in the chocolate matrix but constituted a denser one in the bloom which indicating a phase separation. This was confirmed qualitatively by using high performance liquid chromatography and differential scanning calorimetry, where different contents of triacylglycerols and melting behavior were observed in the bloom and the chocolate matrix. Moreover, polymorphism translation from β' form to β form appeared in the bloom but did not in the chocolate matrix, which suggesting that polymorphism translation is the result rather than the cause of bloom formation.

Keywords Bloom · CBS compound chocolate · Composition · Morphology · Melting behavior

F. Wang · Y. Liu · L. Shan · Q. Jin · X. Wang (✉) · L. Li
State Key Laboratory of Food Science and Technology,
School of Food Science and Technology, Jiangnan University,
1800 Lihu Road, Wuxi 214122, Jiangsu,
People's Republic of China
e-mail: wxg1002@hotmail.com

Introduction

Cocoa butter (CB) is an extremely important component of chocolate formulations. However, the historical uncertainty in the cocoa butter supply and the volatility in cocoa butter prices forced confectioners to seek other alternatives. This ensures a continuing need for economical vegetable fats to replace cocoa butter in chocolate and confectionery products [1]. These fats include lauric cocoa butter substitutes (CBS) and non-lauric cocoa butter replacers (CBR). With the growing awareness of health, the use of CBR was increasingly restricted for the high content of trans-fatty acids [1, 2]. Therefore, CBS plays a more important role in the confectionery industry. These fats have physical properties resembling those of CB. An increasing number of reports focuses on the preparation and processing properties of CBS and the corresponding chocolate products [3–8]. An important crude oil feedstock of such confectionery fats is palm kernel oil (PKO), especially being hydrogenated (HPKO) or fractionated (FPKO), which can be used in place of a major part of CB that is present in normal chocolate. However, one of the outstanding problems of these chocolate products is the poor tolerance with CB. Mixing with CB results in a eutectic state which will lead to a softening and phase separation of chocolate products and eventually the formation of bloom. Several theories to explain these blooming phenomena have been proposed [3, 7, 9–11], but so far none seems to be unanimously approved. Williams et al. [3] found that polymorphic transitions cannot explain formation of bloom until the CB content was greater than 40%. Smith et al. [9] reported that the bloom composition was correlated with the storage temperature, and polymorphic transitions from the initial β' phase to the β phase accompanied the formation of bloom

at all temperatures. Researches about the bloom in CBS based chocolate are far from maturity. The mechanism of this bloom formation still requires an in-depth investigation.

The objective of the present work was to investigate the morphology, composition, melting behavior and polymorphic behavior of fresh and bloomed compound chocolate in order to provide a comprehensive analysis on the mechanisms of fat bloom formation.

Experimental Procedures

Preparation and Storage of Chocolates

HPKO was formulated to a compound chocolate recipe, containing about 10% CB in the fat phase, which is a higher than normal content. The recipe was as follows: 46% sugar, 32.6% fat, 14% cocoa powder, 7% skimmed milk powder, and 0.4% soybean lecithin. All of the ingredients were combined in a grinding scattered machine (F2, Sinco, China) and conched for 3 h at 60 °C, after which the maximum particle size was <25 μm, as measured using a fineness gauge. No refining process was carried out on the mixture. The chocolate was molded using plastic molds (31 mm × 23 mm × 12 mm) and allowed to cool in a refrigerator (5 °C) for 0.5 h before demolding. The compound chocolates were conditioned at 25 ± 2 °C with a relative humidity of 60% until bloom phenomenon was observed. In all procedures, care was taken to ensure that the samples were not touched by hand.

Separation of the Bloom

Fat bloom which developed on the surface of the compound chocolates was scraped off meticulously. To minimize contamination of the bloom with underlying chocolate, a knife and a magnifying lens were used to facilitate the removal of the bloom layer. The knife used had a thermally insulated handle to reduce the transfer of heat from the hand to the samples in order to prevent melting of the bloom or chocolate. All of these operations were performed at 20 ± 2 °C in a temperature-controlled laboratory room to reduce the risk of melting the bloom.

Surface Structure of Chocolate

An atomic force microscope (AFM) (Benyuan, China) was used to image the chocolate surface topography. The AFM tips used with an end point radius of 10 nm had a cantilever spring constant of 42 N/m and were oscillated at ~300 kHz. For soft samples, it is critical that microscope tip not damage the surface being scanned but that it still had to contact the surface to obtain high-resolution measurements. Therefore, measurements were performed in a tapping mode in order not to damage the surface [12–14], and both topographic and phase images were taken. The ambient temperature was held at 16 °C to prevent melting and heat damage to the sample under investigation.

Scanning Electronic Microscopy Analyses

Microstructural studies were carried out using a scanning electronic microscopy (SEM) (Quanta-200, FEI Ltd., Netherlands) on fresh and bloomed chocolates. Sectioned samples (20 × 20 mm) were fixed with glutaraldehyde at 4 °C for ~1 day, then transferred into osmium tetroxide for 1 week, after that they were washed with phosphate buffer and ethanol successively. After being dried by using a critical point dryer, the samples were coated with a thin layer of gold for SEM imaging. Triplicate experiments were conducted capturing 12 micrographs per sample (600×, 1,200×, and 2,400×) showing typical micrographs for each sample.

Polarized Light Microscopy Analyses

Samples of bloom, bloomed chocolate matrix, and the fresh chocolate were observed under a polarized light microscopy (PLM) (XP-203, Changfang, China). Photographs were taken with a Canon A640 camera (Canon, Japan). For these analyses, the sugar phase from the samples was removed by dissolving it in water. Three replicates were observed for each type of chocolate and bloom.

Fatty Acid Composition Analyses

The fatty acid composition was determined as fatty acid methyl esters (FAME) by gas chromatography (GC) on a SHIMADZU (Japan) GC-14B apparatus fitted with a flame ionization detector (FID, temperature 250 °C). The operating conditions were as follows: 100 m × 0.25 mm × 0.2 μm SP-2380 column (Chrompack), temperature program from 120 to 175 °C at 8 °C/min and then to 215 °C at 3 °C/min, carrier gas (nitrogen) at 200 kPa. FAMEs were identified on the basis of their retention data [15]. Three replicates were observed for each type of sample.

Triacylglycerol Composition Analyses

TAGs were separated by high-performance liquid chromatography (HPLC). A Symmetry RP-C18 column (150 mm × 4.6 mm i.d.) was eluted with acetonitrile/dichloromethane (65:35, v/v) at a constant flow rate of 1.0 mL/min. The elution was passed through an evaporative

light-scattering detector (ELSD) with a drift tube temperature of 50 °C. Each sample was analyzed in triplicate and mean values and standard deviations reported.

TAGs were identified by HPLC coupled with an atmospheric pressure chemical ionization (APCI) mass spectrometer (MS) according to the method of Jin et al. [16]. The HPLC conditions were the same as described in the preceding paragraph. A Waters Platform ZMD 4000 (San Jose, CA, USA) mass spectrometer equipped with an APCI interface was set at APCI corona and cone voltages of 3,550 and 57 V, respectively, APCI source block and probe temperatures of, respectively, 100 and 400 °C, and a mass spectrometer multiplier voltage of 700 V.

Melting Properties

Melting curves of the bloom and compound chocolate were obtained by using a PYRIS-1 differential scanning calorimeter (DSC) (Perkin Elmer, USA). Calibration was performed with indium and octadecane. Samples of the compound chocolate were taken from the center of the chocolate bar. Samples were accurately weighed and hermetically sealed in aluminum pans with an empty pan serving as a reference. The melting curve was then obtained by heating the samples from 20 to 60 °C at 5 °C/min. Onset temperature (T_{onset}), peak temperature (T_{peak}), end temperature (T_{end}) and enthalpy of melting (ΔH_{melt}) were calculated automatically by the software. Each sample was analyzed in triplicate and mean values and standard deviations reported.

X-Ray Diffraction Analyses

X-ray diffraction (XRD) analyses were conducted on a D8 Advance X-ray diffractometer (Bruker, Karlsrube, Germany) using Cu-Kα radiation ($\kappa = 1.5406$ Å, voltage 40 kV, current 30 mA, fixed 1.0°, 1.0°, and 0.1 mm divergence, anti-scatter and receiving slits, respectively). Scans from 1° to 30° 2θ were performed at ambient temperature. To eliminate the interference of sugar crystals, the fat phase of the compound chocolate was removed according to the method of Cebula and Ziegleder [17]. Samples were chopped with a knife and then sifted to obtain particle sizes of less than 0.5 mm. The resulted powder was then mixed with 500 mL of cold water, shaken and allowed to stay at room temperature for 4 h. The insoluble material including the fat phase was recovered by vacuum filtration. Each sample was analyzed in triplicate.

Results and Discussion

Surface Properties of Compound Chocolate

Fat crystals evenly distributed on the fresh chocolate with a smooth surface (Fig. 1a). However, some convexities and pits appeared in the surface (the darker parts in the topographic image), which maybe the pores between fat crystals. After long time storage, visible surface bloom gradually developed, which was characterized by the loss of initial gloss of surface that led to a marble like appearance (Fig. 1b). The topographic images revealed

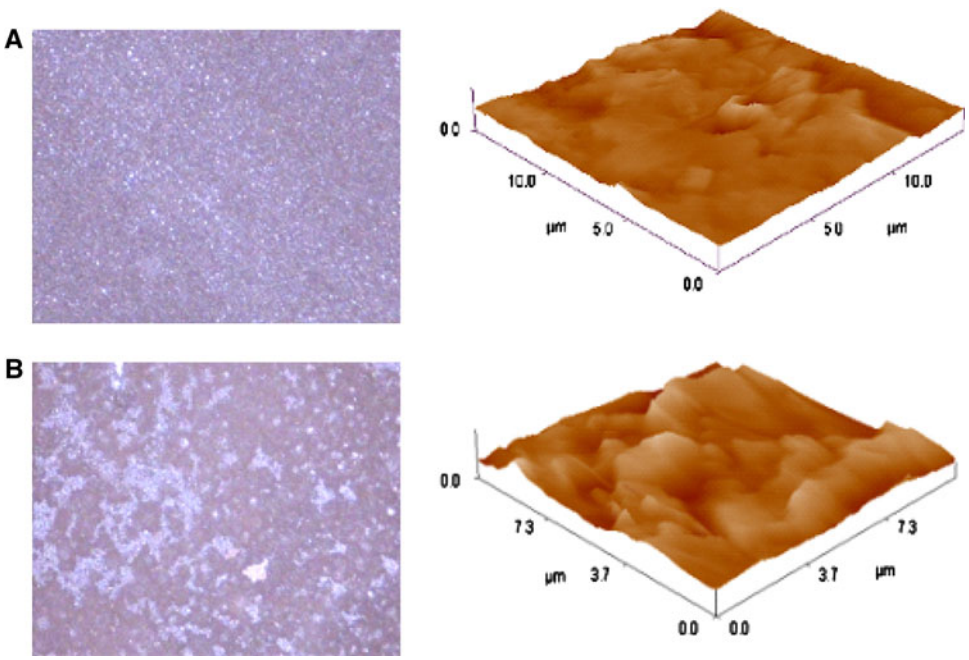

Fig. 1 Surface maps and topographic images of fresh compound chocolate and bloomed chocolate surfaces **a** fresh compound chocolate, 15 × 15 μm; **b** bloomed chocolate, 11 × 11 μm

that the structure of the chocolate surface had changed significantly (Fig. 1b). Surface roughness of the compound chocolate increased from 152 nm (fresh chocolate) to 168 nm (bloomed chocolate). Bearing analysis showed a shift in the upper 50% height frequency distribution from 0.69–1.14 μm to 0.73–1.25 μm. Larger fat crystals were visible on the surface of bloomed chocolate compared with the fresh chocolate. There was an apparent growth in the size of surface features which correlated with the visual appearance of the bloom.

The pore structure were also found in other kinds of chocolate [13, 18, 19], and was postulated to open up into channels which are responsible for liquefied fat transport and subsequent promotion of fat bloom formation. However, how do these pores work in CBS chocolate, and whether they are in line with other chocolates is not yet known. In-depth study will be done in future work.

SEM

Microstructural examination using SEM showed remarkable variations in crystalline network structure, inter-crystal connections and spatial distributions of network mass among fresh chocolate, non-bloom and bloom areas of bloomed chocolate (Fig. 2).

Fresh chocolate showed a relative evenly spatial distribution of a dense crystalline network with well defined inter-crystal connections within the structure (Fig. 2a). The dispersed phase particles (Cocoa powder, sugar, etc.) were uniformly dispersed within the crystal network. However, small pores coexisted with the network structure as mentioned in the AFM analysis.

The fat crystal network structure in the non-bloom areas of bloomed chocolate had completely disappeared (Fig. 2b). Particles rearranged irregularly in the surface and the well defined inter-crystal connections disappeared. The dispersed phase particles were directly exposed to the environment. Fat content seemed to have decreased significantly. Bloom areas showed distinct differences compared with non bloom areas (Fig. 2c). Fat crystals were totally covered by the dense inter-crystal connection. The chocolate surface displayed a dense network, even more than the fresh chocolate, which totally covered the dispersed phase particles. It was speculated that a fat migration and accumulation on the

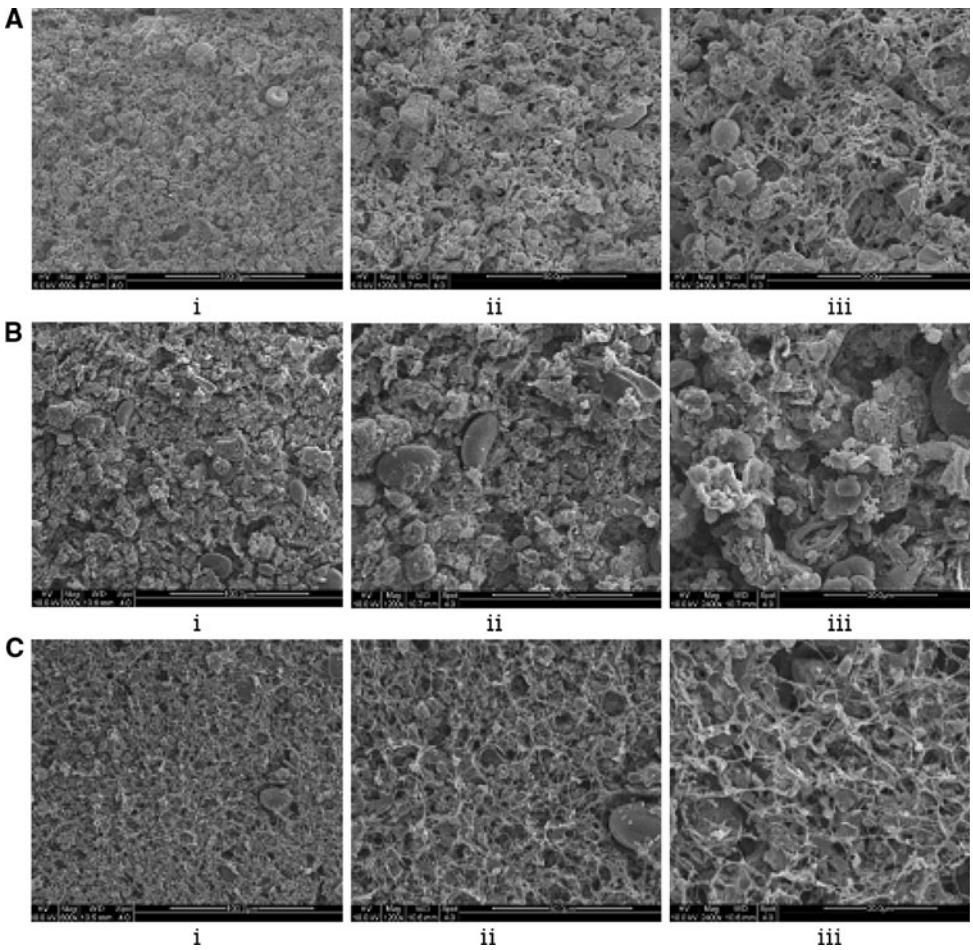

Fig. 2 Scanning electron micrographs (SEM) showing crystalline network microstructures at magnifications of (*i*) ×600, (*ii*) ×1,200, (*iii*) ×2,400, for **a** fresh chocolate, **b** non-bloom areas in bloomed chocolate, **c** bloom areas in bloomed chocolate

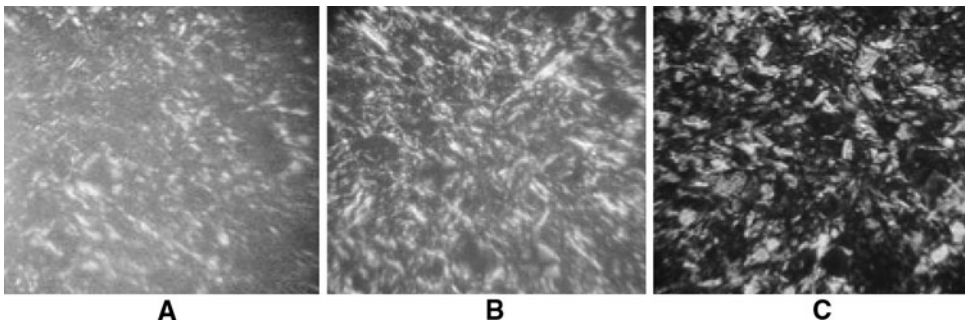

Fig. 3 PLM graphs of chocolate sample **a** fresh chocolate; **b** bloomed chocolate matrix; **c** bloom

surface had happened during the storage of chocolate. These changes may be related to the phase separation, polymorphic transformation, nucleation and growth of new large crystals in a more stable polymorphic form, inducing formation of solid bridges with weak and fewer inter-crystal connections within the crystalline structure [20].

PLM

The different samples were observed under a polarized light microscope (PLM) to verify the AFM and SEM results. Under the PLM, sugar and fat crystals exhibit polarization, whereas cocoa powder solids (amorphous) do not. Therefore, sugar was removed from the samples by dissolving it in water before observation.

Microscopy of the fresh chocolate, bloomed chocolate matrix and bloom are presented in Fig. 3a–c. Each sample exhibited polarization corresponding to the bright white spots on the micrographs. Fresh chocolate presented small, evenly distributed fat crystals with a needle like shape, among which were the dense inter-connections within the crystal network (the white region of the graph) (Fig. 3a). The bloomed chocolate matrix displayed large, tubular crystals among the fat crystal network, which was different from the SEM results (Fig. 3b). It was speculated that, after sugar crystals had been dissolved by water, the fat crystal connection became stronger. Microscopy of bloom showed the biggest crystals of various shapes, such as "bow-tie", needle-like and spherules crystals (Fig. 3c). Therefore, the speculation of crystal growth and formation of new crystals was confirmed.

Fatty Acid Compositions

The bloom and the compound chocolate showed obvious differences in their fatty acid compositions, with the former containing a higher content of lauric acid ($C_{12:0}$), stearic acid ($C_{18:0}$), and oleic acid ($C_{18:1}$) and a lower content of myristic acid ($C_{14:0}$) and palmitic acid ($C_{16:0}$) (Table 1). But these differences in fatty acid compositions were not sufficient to describe the compositional differences between the bloom and the compound chocolate.

Table 1 Fatty acid compositions of bloom and compound chocolate (%)

FA	Bloom	Compound chocolate
C8:0	1.3	1.5
C10:0	2.6	2.5
C12:0	52.5	45.7
C14:0	15.6	21.2
C16:0	7.9	11.1
C18:0	10.5	9.6
C18:1	5.8	3.8
Others	3.8	4.6

Table 2 TAG compositions of bloom and compound chocolate (%)

TAG	Bloom	Compound chocolate	Percentage content changes[a] (%)
LLL	29.7	26.0	12.5
LLM	19.9	26.7	−34.2
LMM/LLP	8.6	15.0	−74.4
MMM	4.8	8.4	−75.0
LPP	2.2	4.3	−95.5
MPP	1.6	2.8	−75.0
POP	5.3	3.8	28.3
POS	15.3	4.7	69.3
SOS	10.0	4.8	52
Trisaturated[b]	66.8	83.2	−19.7
Monounsaturated[c]	30.6	13.3	130.1

C canoic acid, *L* lauric acid, *M* myristic acid, *O* oleic acid, *P* palmitic acid, *S* stearic acid

[a] Percentage content changes calculated according to the following formula: Percent contents changes $= \frac{A-B}{B} \times 100\%$ where A refers to content of specific TAG in bloom; B refers to content of corresponding TAG in compound chocolate

[b] Trisaturated = LLL, LLM, LMM/LLP, MMM, LPP, MPP

[c] Monounsaturated = POP, POS, SOS

TAG Compositions

The main TAGs in bloom and compound chocolate were almost in the same amounts (Table 2). However, the

content of certain TAGs in bloom were significantly different from that in compound chocolate which confirmed the occurrence of phase separation. This means that some TAGs in chocolate had migrated from the center to the surface of chocolate. The content of trisaturated (SSS) TAGs was reduced by 19.7%, while the content of symmetrical monounsaturated TAGs was raised by 130.1%, compared with the compound chocolate. Interestingly, the content of trilaurin (LLL) was raised by 12.5% although other trisaturated TAGs were remarkably reduced. It seems there was a close correlation between bloom and TAGs species.

As we know, CB is composed predominantly (>75%) of symmetrical triacylglycerols with oleic acid in the 2-position (POP, POS, SOS) while CBS contains trilaurin as the main TAG. After hydrogenation, CBS is composed nearly all of trisaturated TAG. Therefore, the bloom was still a mixture of these two fats. However, it was obvious that the bloom formation had a important relationship with the poor compatibility between HPKO and CB [10].

Melting Properties

The melting behavior of the bloom was remarkably different from that of the compound chocolate samples (Fig. 4). The melting curve of fat bloom showed a sharper melting peak at 31.9 °C with the highest melting enthalpy (72 J/g), while the compound chocolate showed double peaks at 26.9 and 34.7 °C with small melting enthalpies (5.51 and 14.76 J/g, respectively) (Table 3), which means a phase separation appeared in the chocolate during storage. From the TAG analysis we can speculate that long chain trisaturated TAG stayed in the chocolate matrix which corresponding the melting peak at 34.7 °C while symmetrical TAG and other trisaturated TAG migrated to surface showed the sharper melting peak.

Table 3 Melting properties of bloom and compound chocolate

Sample	T_{onset} (°C)	T_{peak} (°C)	T_{end} (°C)	ΔH_{melt} (J/g)
Bloom	28.4 ± 0.4	31.9 ± 0.1	33.9 ± 0.3	72.01 ± 0.84
Compound chocolate				
Peak 1	23.8 ± 0.2	26.9 ± 0.3	28.5 ± 0.2	5.51 ± 0.24
Peak 2	31.4 ± 0.4	34.7 ± 0.3	36.2 ± 0.1	14.76 ± 0.32

Mean values from triplicate analysis ± standard deviation

X-Ray Diffraction

Both long and short spacing of the X-ray diffraction graph of the bloom were observed (Fig. 5). The long spacing X-ray diffractograms indicate typical lamellar packing structures of fats. The polymorphic behavior of the bloom comprised two very strong peaks at 37.40 and 31.8 Å, a medium one at 12.62 Å, and 2 weak ones at 18.94 and 10.77 Å, respectively (Fig. 5a). At the same time, only three peaks appeared in the compound chocolate at 36.70, 12.62, and 18.94 Å, respectively (Fig. 5b). This indicated difference in long spacing pattern between bloom and compound chocolate. Therefore, the lamellar packing state of TAGs in the bloom had undergone changes to a certain extent as compared with compound chocolate.

The short spacing X-ray diffractograms indicate polymorphic forms of fat crystals. There was a significant difference between the short spacing X-ray diffractograms of bloom and compound chocolate. The fat crystals of compound chocolate showed two weak peaks at 4.21 and 3.80 Å corresponding to the β' polymorph. The bloom

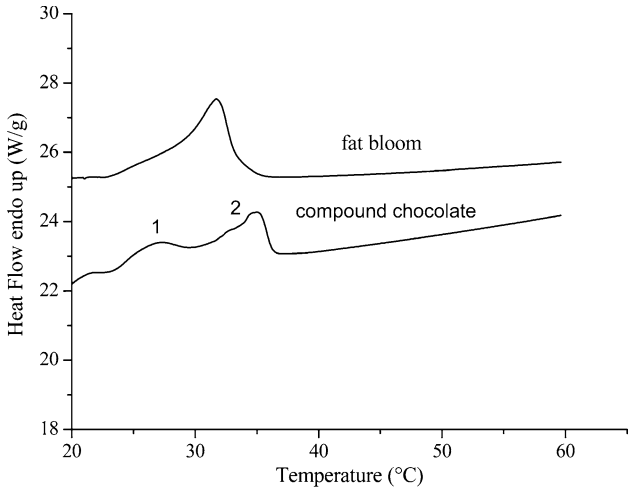

Fig. 4 Melting curves of compound chocolate and the associated bloom

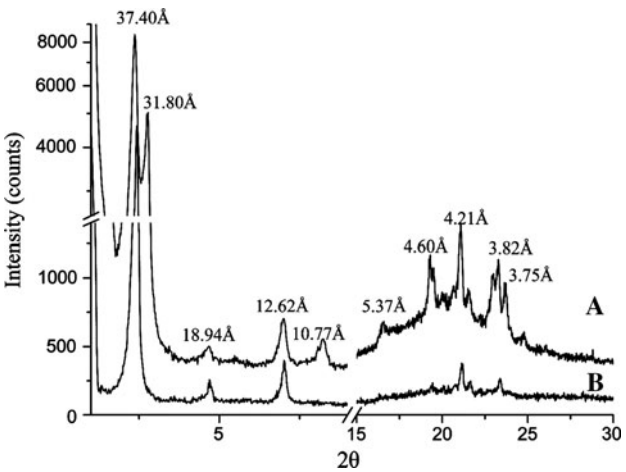

Fig. 5 X-ray diffraction grams of **a** bloom and **b** compound chocolate

showed multiple relative stronger peaks at 4.60, 4.21, 3.82, and 3.75 Å which was attributed to a mixture of the β form and the β' form crystals. Thus, a translation from β' polymorph to β polymorph had happened on the chocolate surface together with the formation of bloom while no polymorphism translation happened in the chocolate matrix.

Conclusion

The phase separation was confirmed in our research. Both CB and lauric fats existed in the bloom, but the migration degree of CB maybe higher than the lauric fats. The migration fats accumulated on the surface and then re-crystallization into more stable forms. Moreover, polymorphism translation from the β' form to β form was only found in the surface bloom while not in the chocolate matrix. Therefore, polymorphism translation was the result rather than the cause of bloom formation.

Acknowledgments The work is supported by the National High Technology Research and Development Program (863 Program) of China (Contract No: 2010AA101506). We also express our gratitude to the PhD research fund of Jiangnan University for their financial support.

References

1. Bailey's industrial oil and fat products. New Jersey (2005)
2. Judd JT, Clevidence BA, Muesing RA, Wittes J, Sunkin ME, Podczasy JJ (1994) Dietary *trans* fatty acids: effects on plasma lipids and lipoproteins of healthy men and women. Am J Clin Nutr 59:861–868
3. Williams SD, Ransom-Painter KL, Hartel RW (1997) Mixtures of palm kernel oil with cocoa butter and milk fat in compound coatings. JAOCS 74:357–366
4. Rossell JB (1985) Fractionation of lauric oils. JAOCS 62:385–390
5. Pease JJ (1985) Confectionery fats from palm oil and lauric oil. JAOCS 62:426–430
6. Laning SJ (1985) Chemical interesterification of palm, palm kernel and coconut oils. JAOCS 62:400–407
7. Sabariah S, Ali ARM, Chong CL (1998) Chemical and physical characteristics of cocoa butter substitutes, milk fat and Malaysian cocoa butter blends. JAOCS 75:905–910
8. Ransom-Painter KL, Williams SD, Hartel RW (1997) Incorporation of milk fat and milk fat fractions into compound coatings made from palm kernel oil. J Dairy Sci 80:2237–2248
9. Smith KW, Cain FW, Talbot G (2004) Nature and composition of fat bloom from palm kernel stearin and hydrogenated palm kernel stearin compound chocolates. J Agric Food Chem 52:5539–5544
10. Lonchampt P, Hartel RW (2004) Fat bloom in chocolate and compound coatings. Eur J Lipid Sci Technol 106:241–274
11. Hartel RW (1996) Applications of milk-fat fractions in confectionery products. JAOCS 73:945–953
12. Yang H, Wang Y, Lai S, An H, Li Y, Chen F (2007) Application of atomic force microscopy as a nanotechnology tool in food science. J Food Sci 72:R65–R75
13. Hodge SM, Rousseau D (2002) Fat bloom formation and characterization in milk chocolate observed by atomic force microscopy. JAOCS 79:1115–1121
14. Rousseau D (2006) On the porous mesostructure of milk chocolate viewed with atomic force microscopy. LWT 39:852–860
15. Shen Z, Birkett A, Augustin MA, Dungey S, Versteeg C (2001) Melting behavior of blends of milk fat with hydrogenated coconut and cottonseed oils. JAOCS 78:387–394
16. Jin Q, Gao H, Shan L, Liu Y, Wang X (2007) Study on grainy crystals in edible beef tallow shortening. Food Res Int 40:909–914
17. Cebula DJ, Ziegleder G (1993) Studies of bloom formation using X-ray diffraction from chocolates after long-term storage. Fat Sci Technol 9:340–343
18. Smith PR, Dahlman A (2005) The use of atomic force microscopy to measure the formation and development of chocolate bloom in pralines. JAOCS 82:165–168
19. Quevedo R, Brown C, Bouchon P, Aguilera JM (2005) Surface roughness during storage of chocolate: fractal analysis and possible mechanisms. JAOCS 82:457–462
20. Afoakwa EO, Paterson A, Fowler M, Vieira J (2009) Influence of tempering and fat crystallization behaviours on microstructural and melting properties in dark chocolate systems. Food Res Int 42:200–209